PREFERRED ORIENTATION IN NONCRYSTALLINE POLYMERS

W. RULAND and W. WIEGAND
Fachbereich Physikalische Chemie-Polymere-D-3550 Marburg/Lahn, Germany

INTRODUCTION

The determination of the orientational anisotropy is an essential part of the characterization of polymer structures and their relationship to physical properties. There are a number of methods in use to determine orientation parameters (X-ray diffraction, light scattering, optical birefringence, IR dichroism, NMR, and fluorescence polarization) which are sensitive to the orientation of various components of the polymer structure (chain segments, crystallites, amorphous domains, lamellar structures, and spherulites) and which result in various types of orientation parameters. In general, these methods can be grouped into two classes, those which describe orientation in terms of angular distributions (e.g., pole figures) and those which result in the determination of weighted averages (e.g., moments) of these distributions. Angular distributions are obtained mainly by scattering methods (X-ray, electron, neutron, light scattering), whereas moments of these distributions are obtained by measurements of physical properties which can be related to tensors of various ranks, the rank determining the order of the moments. Since angular distributions contain generally more information than a limited number of moments of these distributions, especially since mostly only second moments and, less frequently, fourth moments are determined, we shall confine our discussion mainly to the problems related to the determination of angular distributions and, in particular, those occurring in the studies of preferred orientation of noncrystalline structures.

THEORETICAL

The orientation of the crystals in a polycrystalline material is conveniently described by the distribution $w(\alpha,\beta,\gamma)$ of the Euler angles α, β, γ which define the orientation of the crystal-fixed coordinate systems with respect to a sample-fixed system of axes. Diffraction methods result in the determination of the angular distributions (pole figures) $g_{hkl}(\varphi,\psi)$ of the normals of the plane of index (hkl) with respect to this sample-fixed coordinate system. It has been shown by Roe [1] that, in principle, an infinite number of plane-normal distributions is necessary to compute $w(\alpha,\beta,\gamma)$ using an inversion method based on series of

Journal of Polymer Science: Polymer Symposium 58, 43–58 (1977)
© by John Wiley & Sons, Inc.

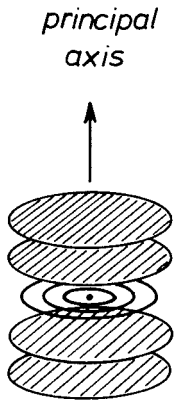

FIG. 1. Correlation function for a turbostratic (smectic) structure.

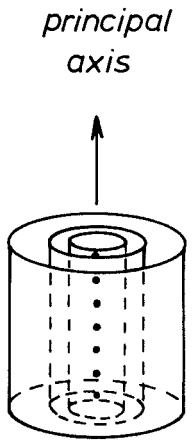

FIG. 2. Correlation function for a nematic structure.

spherical harmonics. The problem becomes, however, much simpler if one considers a system with cylindrical symmetry of the orientation of the crystallites about a sample-fixed principal axis (fiber structure) and a random rotation of the crystallites about a crystal-fixed principal axis (e.g., the main axis of the polymer chains). In this case, the orientation is completely defined by the distribution $g(\varphi)$ of the principal axes of the crystallites with respect to the principal axis of the sample.

Such an assumption is a convenient starting point to discuss the problems occurring in the determination of preferred orientation in noncrystalline materials.

When studying preferred orientation in a noncrystalline material by diffraction methods the main problem consists in defining the structural units, the orientation of which causes the anisotropy of the scattering. There are two types of short-range order for which a theoretical treatment of the preferred orientation is relatively easy: turbostratic (smectic) structures and nematic structures.

A turbostratic structure consists of a parallel stacking of layers with relatively

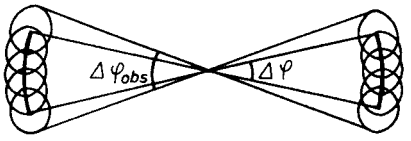

FIG. 3. Effect of the tangential width on the angular distribution of an (hkl) interference line.

perfect internal structure in which the layers are randomly rotated and translated with respect to each other so that no positional correlation exists between atoms belonging to different layers except the overall parallelism. The correlation function for such a structure is shown in Figure 1. The correlation function consists of a series of concentric rings in a plane through the origin and a periodic series of layers with constant surface density parallel to this plane. A nematic structure consists of a parallel stacking of rods with relatively perfect internal structure. The rods are randomly rotated and translated with respect to each other so that no positional correlation exists between atoms belonging to different rods except the overall parallelism. The correlation function for such a structure (considered to be rotated about its principal axis) is shown in Figure 2. The correlation function consists of a periodic series of narrow distributions on a straight line through the origin and a series of concentric cylinder walls with constant surface density.

The intensity distribution in reciprocal space of the turbostratic structure is similar to the correlation function of the nematic structure and vice versa, i.e., ($00l$) interference peaks and (hk) cylinder walls for the turbostratic structure, ($hk0$) interference rings and (l) layers in the case of a nematic structure. In the case of random orientation, the turbostratic structure shows symmetrical ($00l$) line profiles and asymmetrical (hk) line profiles of the type

$$I_{hk}(s) = 1/2\pi s\sqrt{s^2 - s_{hk}^2} \quad s \geq s_{hk} \tag{1}$$

(von Laue, [2]), the nematic structure shows symmetrical ($hk0$) line profiles and asymmetrical (l) line profiles of the type

$$I_l(s) = 1/2s \quad s \geq s_l \tag{2}$$

where $s = 2 \sin \theta/\lambda$, s_{hk} and s_l are the absolute values of the reciprocal lattice vectors related to the internal structure of the layers and the rods, respectively. Finite size and perfection of the internal structure will, of course, introduce a supplementary broadening of $I_{hk}(s)$ and $I_l(s)$ which affects, however, essentially only the s values in the vicinity of s_{hk} or s_l.

If one considers a nonrandom orientation, there is obviously an essential difference between the effect of orientation on the intensity distributions of the ($kh0$) and ($00l$) lines on one hand, and the (hk) and (l) lines on the other.

The effect of preferred orientation on the ($hk0$) and ($00l$) lines is in principle the same as that on an interference peak of a three-dimensionally ordered structure. However, since the size and the perfection of the turbostratic and nematic domains are, in general, relatively small, the observed pole figures can contain a nonnegligible contribution from the finite width of the lines tangential to the radius vector $\mathbf{s}_{hkl}$ (see Figure 3). This effect has been discussed in an earlier paper (Ruland, [3]) where it was shown that it can be considered as a convolution

of $g(\varphi)$ with a broadening function, and a general elimination procedure using Fourier series has been proposed and applied to a series of orientation measurements of turbostratic structures (carbon fibers). In order to assess the magnitude of the effect, let us assume the tangential line profile to be Lorentzian and the angular distribution of the center of the line to be given by

$$g(\varphi) = \frac{1 - q^2}{1 + q^2 - 2q \cos 2\varphi} \tag{3}$$

where q is an orientation parameter varying from 0 to 1 for an orientation varying from random to perfect orientation at $\varphi = 0$, and from 0 to -1 for an orientation varying from random to perfect at $\varphi = 90°$. Considering the orientation parameter

$$f = \tfrac{1}{2}(3\langle\cos^2\varphi\rangle - 1)$$

one can show that

$$f = 1 - \tfrac{3}{2}F(q)$$

with

$$F(q) = \frac{1 + q}{4\sqrt{q}\ \operatorname{artanh}\sqrt{q}} - \frac{(1 - q)^2}{4q}$$

For negative values of q, $F(q)$ is, to a good approximation, a linear function of q:

$$F(q) \simeq \tfrac{1}{3}(2 - q) \quad -1 < q < 0$$

which means that f is approximately $q/2$ for this type of orientation. For $q > 0$, the above approximation still holds reasonably well for $0 < q < 0.3$; for q values higher than 0.5 an approximation of the type

$$f = 1 - \frac{3}{2 \ln [4/(1 - q)]}$$

can be used.

The choice of a $g(\varphi)$ in the form of eq. (3) for calculating the effect of the tangential width on the observed $g(\varphi)$ has the advantage that this function can be considered as an infinite period series of Lorentzian distributions

$$g(\varphi) = \sum_n L(q, \varphi - n\pi)$$

for $0 < q < 1$ and

$$g(\varphi) = \sum_n L\left(q, \varphi - \frac{2n + 1}{2}\pi\right)$$

for $-1 < q < 0$ where

$$L(q,\varphi) = 2\left(\ln\frac{1}{|q|}\right)\frac{1}{\ln^2\left(\frac{1}{|q|}\right) + 4\varphi^2}$$

with an integral width

$$B_L(q) = \frac{\pi}{2} \ln \frac{1}{|q|}$$

If the line profile due to finite size and imperfection of the domains has the integral width $B(s)$ in $s = 2 \sin \theta/\lambda$, and if $B(s)$ is still small compared with s_{hkl}, its effect on $g(\varphi)$ can, to a first approximation, be considered as due to a broadening in φ with a width $B(\varphi) = B(s)/s_{hk0}$ or $B(s)/s_{00l}$, respectively. If this broadening is due to a Lorentzian distribution, the observed angular distribution is still of the type given in eq. (3) but has a smaller value of q given by the equation

$$q_{\text{obs}} = q \left(1 - \frac{2B_s}{\pi s_{hkl}}\right)$$

since

$$B_s \ll s_{hkl}.$$

For $-0.5 < f < 0.2$ this means, to a first approximation

$$f_{\text{obs}} \simeq f \left(1 - \frac{2B_s}{\pi s_{hkl}}\right), \tag{4}$$

and for $f \simeq 1$:

$$f_{\text{obs}} \simeq 1 - \frac{3}{2 \ln (2\pi s_{hkl}/B_s)}$$

For disordered structures of the kind considered here, $2B_s/(\pi s_{hkl})$ can be expected to be of the order of 0.1, the error in f is thus about 10% for f values below 0.2, increasing gradually to about 40% with respect to f, i.e., nearly 70% with respect to f_{obs}, when f tends towards unity (Fig. 4).

This shows, that the error can become considerable especially if the preferred orientation of $\mathbf{s}_{hkl}$ is along the primary axis, i.e., layers perpendicular to this axis in the turbostratic case and rods perpendicular to this axis in the nematic case. It is thus of interest to include the (hk) and the (l) interference in the determination of the preferred orientation since these interferences can be used to assess the tangential width of the $(00l)$ or $(hk0)$ lines, respectively, and their spacial distribution contains information on $g(\varphi)$, although in a more complicated way.

For (hk) interferences, this problem has been treated in an earlier paper (Ruland and Tompa, [4]). It was shown that the intensity distribution $I_{hk}(\mathbf{s})$ can be taken as a product of the isotropic distribution $I_{hk}(s)$ given in eq. (1) and a function $F(\sigma,\varphi)$

$$I_{hk}(\mathbf{s}) = I_{hk}(s) \cdot F(\sigma,\varphi) \tag{5}$$

in which $\sin \sigma = s_{hk}/s$ and

$$F(\sigma,\varphi) = 2 \int_0^{\pi} g(\beta) d\eta \tag{6}$$

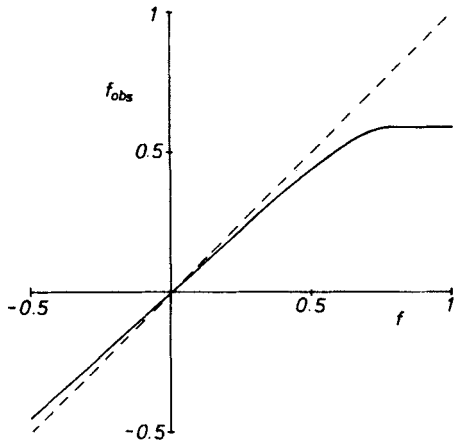

FIG. 4. The observed orientation parameter f_{obs} as a function of the correct parameter f for $B_s/s_{hkl} = 0.16$.

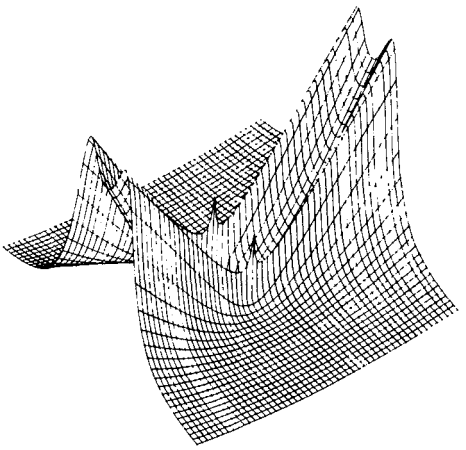

FIG. 5. The two-dimensional profile of the function $F(\sigma,\varphi)$ in the plane containing the principal axis ($\sin\sigma = s_{hk}/s$, $q = 0.8$).

where $g(\beta)$ is the normalized orientation distribution of the principal axis as a function of the angle β related to σ, η, and φ through

$$\cos\beta = \cos\varphi\cos\sigma + \sin\varphi\sin\sigma\cos\eta$$

The function $F(\sigma,\varphi)$ can be obtained in a closed form for orientation distributions of the type given in eq. (3).

Figures 5 and 6 show perspective plots of the two-dimensional profiles of $F(\sigma,\varphi)$ for $q = 0.8$ and -0.8, respectively, as functions of s in the plane containing the primary axis, the latter being parallel to the projection onto this plane of the lines running from the lower left to the upper right hand side of the diagrams. An inspection of the diagrams shows that pronounced maxima are observed at $\varphi = 90°$ for positive q values and $\varphi = 0°$ for negative q values, i.e., at right angles to the maxima of the corresponding $g(\varphi)$ functions. In contrast to the effect of preferred orientation on (hkl) interferences the (hk) interferences [and the (l)

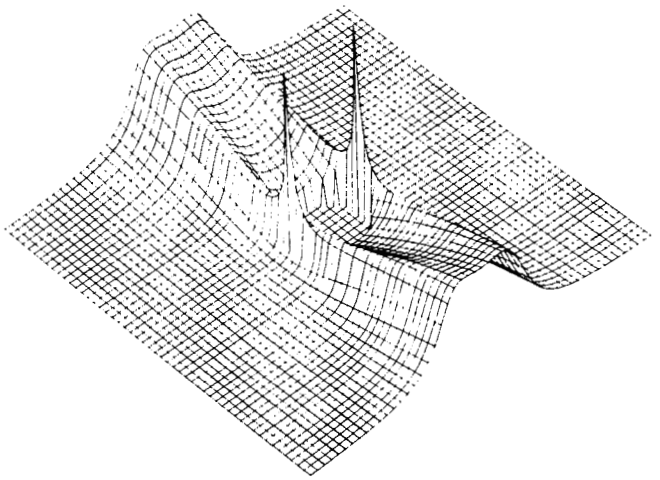

FIG. 6. The two-dimensional profile of the function $F(\sigma,\varphi)$ in the plane containing the principal axis ($\sin\sigma = s_{hk}/s$, $q = -0.8$).

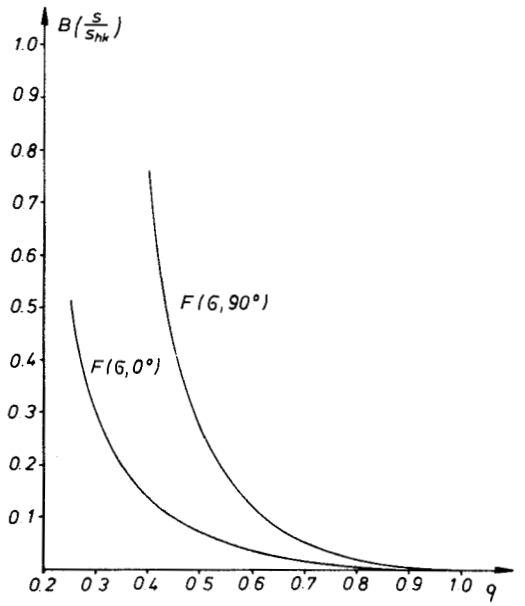

FIG. 7. Half-peak width in s/s_{hk} of $F(\sigma,0)$ and $F(\sigma,90°)$ as a function of $|q|$.

interferences, as will be demonstrated later] show a variation of the intensity in φ as well as in s. This means that the profile of an (hk) interference in s at constant φ is a function of $g(\varphi)$. The most simple relationships for such profiles are obtained for $\varphi = 0°$ and $\varphi = 90°$, respectively,

$$F(\sigma,0) = 2\pi g(\sigma) \tag{7}$$

$$F(\sigma,90°) = \frac{\sqrt{q}}{\operatorname{artanh}\sqrt{q}} \frac{1}{[(1+q)^2 - 4q\sin^2\sigma]^{1/2}} \tag{8}$$

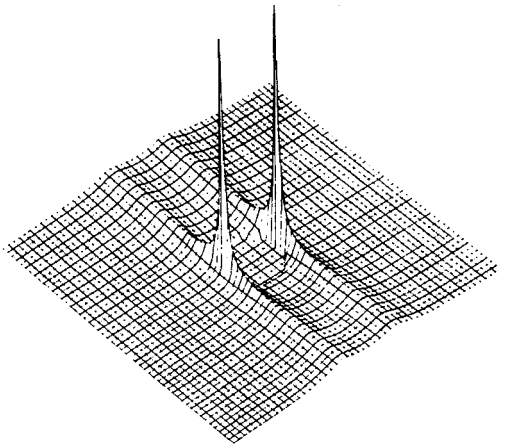

FIG. 8. The two-dimensional profile of the function $F(\sigma,\varphi)$ in the plane containing the principal axis ($\cos\sigma = s_l/s$, $q = 0.8$).

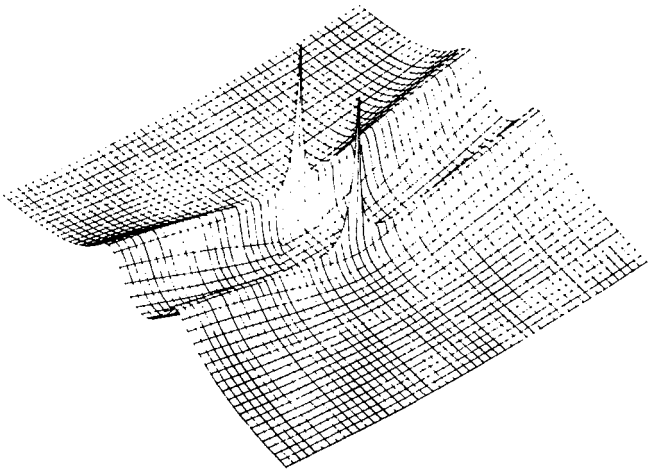

FIG. 9. The two-dimensional profile of the function $F(\sigma,\varphi)$ in the plane containing the principal axis ($\cos\sigma = s_l/s$, $q = -0.8$).

Figure 7 shows the variation of the half-peak width in s/s_{hk} of the line profiles in $F(\sigma,0)$ for negative q values and in $F(\sigma,90°)$ for positive q values. It appears that, in both cases, the widths change considerably with q and that the effect is larger in $F(\sigma,90°)$ than in $F(\sigma,0°)$.

If other line broadening effects can be eliminated these relationships should permit a determination of orientation parameters from a quantitative profile study of the (hk) lines.

For nematic structures one can show that the effect of preferred orientation on the (l) interferences leads to an expression similar to eq. (5)

$$I_l(\mathbf{s}) = I_l(s)\cdot F(\sigma,\varphi) \tag{9}$$

where $F(\sigma,\varphi)$ is the same function as in eq. (6) except that the definition of σ is changed to

$$\cos\sigma = s_l/s$$

Figures 8 and 9 show perspective plots of the two-dimensional line profiles of $F(\sigma,\varphi)$ with the above definition of σ for $q = 0.8$ and -0.8, respectively, as functions of **s** in the plane containing the primary axis, the latter being parallel to the projection onto this plane of the lines running from the lower left to the upper right hand side of the diagram. The features of the diagrams are similar to those of Figures 5 and 6, the pronounced maxima are, in contrast to the (hk) lines, at $\varphi = 0°$ for positive q values and at $\varphi = 90°$ for negative q values. The relationships between $|q|$ and the half-peak widths of the profiles in s given in Figure 7 are valid for the (l) lines also provided the change in the sign of the corresponding q values is taken into account.

These theoretical considerations result in the following conclusions: For noncrystalline materials with structural units of turbostratic or nematic type one has to expect two kinds of interference maxima, those which change intensity and line-profile in s with preferred orientation and those which change only in intensity. The latter can be evaluated in the same way as crystalline interferences provided the effect of the tangential width is taken into account. The asymmetry of the profile of the former and its change with preferred orientation can be used to characterize the type of short-range order and to obtain supplementary information on the degree of preferred orientation.

In those cases in which the type of short-range order cannot be decided from a study of the intensity distribution, a Fourier transformation of the total coherent scattering to obtain the orientation dependent pair correlation function is a useful although rather tedious procedure. Its evaluation would consist in determining the angular distribution of the interatomic distances; in favorable cases these may be separated into inter- and intramolecular distances and thus provide information on the orientation of molecular segments and their packing.

Apart from the determination of pole figures, scattering methods can be used to measure the anisotropy of the density fluctuation by studying the angular dependence of the diffuse small-angle scattering near the origin of reciprocal space. In a noncrystalline material the density fluctuations can be considered to be composed of a contribution from thermal motion (phonons) and from the "frozen-in" disorder. Both contributions can show an anisotropy. In the case of thermal motion this is due to the change of the group velocities of longitudinal waves with the propagation direction and thus directly related to the anisotropy of the dynamic modulus of the material. In the case of the "frozen-in" disorder an anisotropy of the diffuse small-angle scattering can be interpreted as due to an anisotropy of the short-range order.

A study of the temperature dependence of this effect can be used to separate the two components.

EXPERIMENTAL

A number of experimental results exist for the effect of preferred orientation on (hk) interferences of turbostratic structures. Such structures develop when organic material is thermally decomposed and small polycondensed aromatic

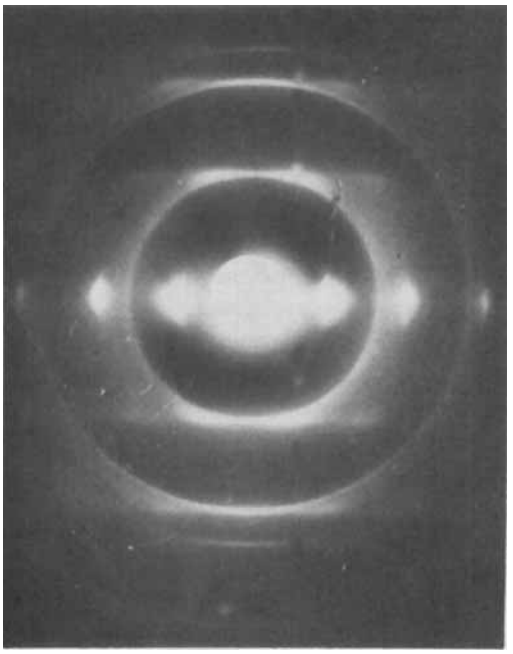

FIG. 10. Electron diffraction diagram of a highly oriented turbostratic structure (carbon fiber).

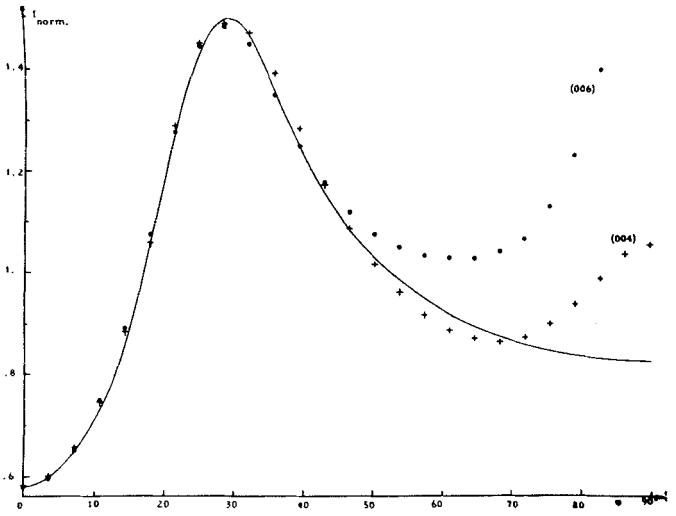

FIG. 11. Comparison of theoretical and experimental values for (hk) interferences measured at constant $s = 1.1s_{hk}$ as a function of φ.

ring systems are formed which develop a tendency towards parallel stacking. The structures obtained can show a preferred orientation of the layer normals in the direction of the principal axis (pyrolytic carbon, Guentert and Cvikevich, [5]) or perpendicular to it (carbon fibers, Ruland and Tompa, [4]; Fourdeux, Perret and Ruland, [6]). Figure 10 shows an electron diffraction diagram of a

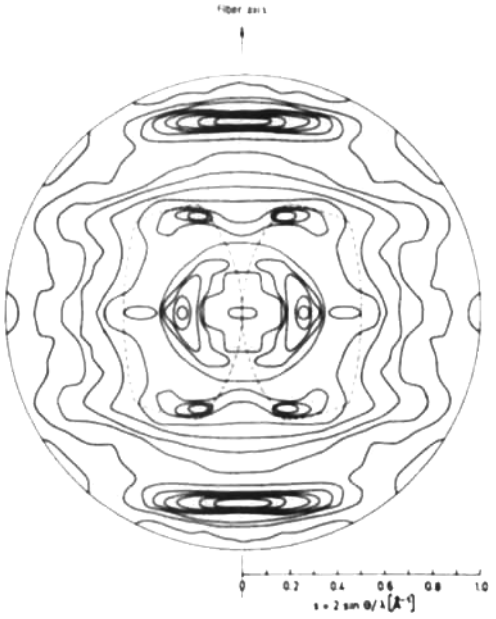

FIG. 12. Diffuse X-ray scattering intensity of polyamide 6 (isointensity lines).

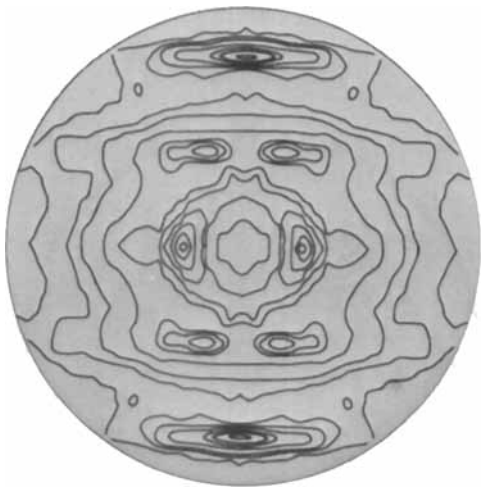

FIG. 13. Diffuse X-ray scattering intensity of polyamide 66 (isointensity lines).

carbon fiber with high preferred orientation. The difference in the intensity distribution between the (00l) lines (on the equator) and the (hk) lines is obvious. Figure 11 shows a plot of the intensity of a (10) and a (11) interference at constant $s = 1.1s_l$ as a function of φ together with a plot of the corresponding

values of $F(\sigma,\varphi)$. The curves show a good agreement between the theoretical and experimental values outside the equatorial region in which the (00*l*) intensities overlap with the (*hk*) intensities.

The effect of preferred orientation on nematic structures in polymers has not yet been studied in detail. This is mainly due to the fact that a neat distinction between nematic and amorphous is rather difficult. If bundles of molecules exist in the amorphous phase of polymers, the structure could be treated as nematic,

FIG. 14. Diffuse X-ray scattering intensity of polyamide 11 (isointensity lines).

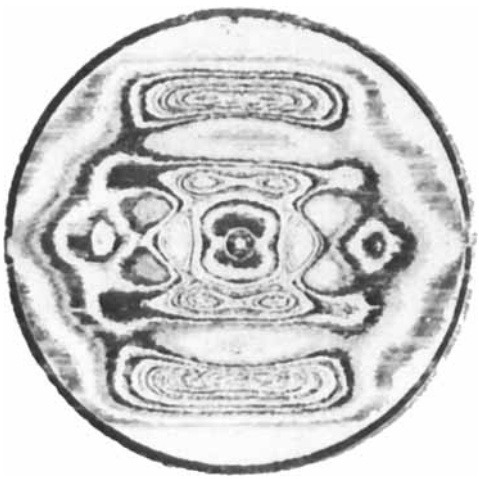

FIG. 15. Diffuse X-ray scattering of an alternating P(ETFE) copolymer (two-dimensional microdensitometer diagram).

provided the domains of anisotropic short-range order are large enough. The results of the neutron small-angle scattering studies on solid solutions of deuterated and undeuterated amorphous polymers seem to exclude the existence of bundle structures in atactic PMMA and polystyrene. However, polyamides, for example, are known to form structures of intermediate order between amorphous and crystalline which, in the oriented state, show intensity distributions very similar to those one would expect for nematic structures with preferred orientation. Figures 12–14 show equal-intensity lines for a series of polyamide fibers with diffuse intensity distributions which appear to be, at least qualitatively, composed of a function of the type given in Figure 8 and, of course, modulations due to the structure factor of the single chain. Similar intensity distributions are observed in the fiber diagrams of an oriented P(ETFE) alternating copolymer with about 10% sequential disorder. A two-dimensional microdensitometer plot is shown in Figure 15. The fact that the structure factor of the single extended molecule is not monotonic in the direction perpendicular to the chain axis makes it more difficult to extract the function $F(\sigma,\varphi)$ from the scattering intensity, in contrast to the case of the carbon fibers, however, this could, in principle, be possible.

A basic problem in the determination of the preferred orientation of the amorphous domains in semicrystalline polymers is the difficulty of finding an unambiguous way to separate the crystalline interferences from the amorphous ones. Figure 16 shows a series of intensity measurements in s at constant φ for a polyethylene film cold stretched about 300%. In the plots, two kinds of separation lines between the crystalline and the amorphous interferences are drawn which result in the two curves of the integrated intensity versus φ shown in Figure 17. The curve with the lower intensity at $\varphi = 90°$ is the result of a separation procedure in which care was taken that the total integrated intensity

$$\int\int I(s,\varphi) \sin \varphi d\varphi ds$$

of the crystalline and the amorphous interferences maintained the ratio calculated from the crystallinity of the sample measured by other methods, whereas the curve with the higher intensity at $\varphi = 90°$ corresponds to an unreasonably low degree of crystallinity. The orientation parameters f_{obs} related to the chain axes deduced from the two curves are +0.455 and +0.484, respectively, which become +0.540 and +0.575 after a correction using eq. 4 with $B_s/s \simeq 0.25$. The lower value of f can be considered the most probable; in combination with the value of $f = 0.936$ calculated for the crystalline domains it agrees well with the value measured for the optical birefringence.

Figure 18 shows, for the same sample, the variation of the diffuse small-angle scattering extrapolated to $s = 0$ as a function of φ at three different temperatures. The extrapolation has been carried out from the low-angle tail of the amorphous halo excluding the region in which the boundaries between crystalline and amorphous domains determine the small-angle scattering. The spherical averages of these functions are overall density fluctuations within the crystalline and amorphous domains which can be considered to be composed of a component due to structural disorder and a component due to thermal motion. At 4 K, the contribution of the latter component can be neglected so that only the structural

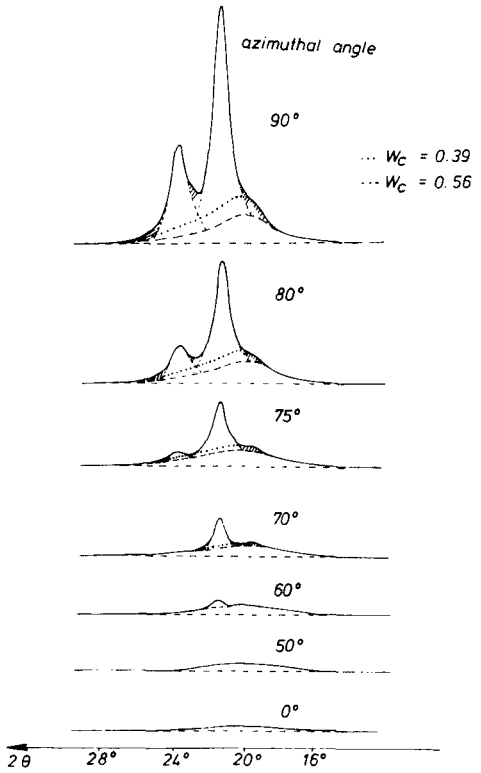

FIG. 16. X-ray scattering intensity of an oriented PE film as a function of s for constant φ.

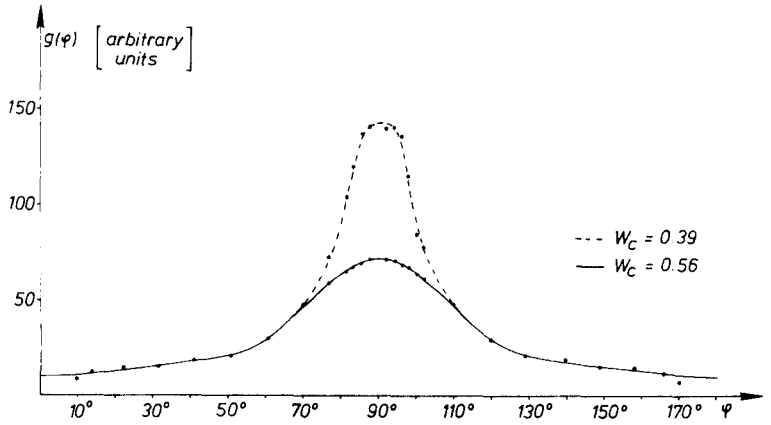

FIG. 17. Orientation function $g(\varphi)$ for the amorphous halo according to two different separation procedures.

disorder is determining the intensity values. It has been shown (Rathje and Ruland, [7]) that the amorphous domains produce the main contribution to these values, and since these domains are oriented one would expect a variation in φ if the short-range order in the amorphous domains is strongly anisotropic. Inspection of Figure 18 shows that this seems not to be the case. This result could

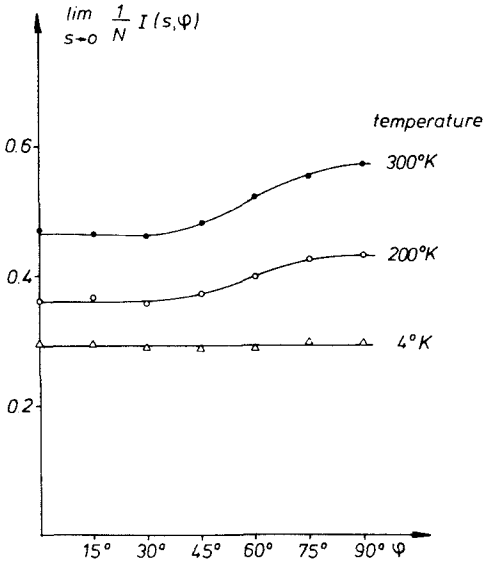

FIG. 18. Diffuse X-ray scattering of an oriented PE film extrapolated towards zero scattering angle as a function of φ for three different temperatures.

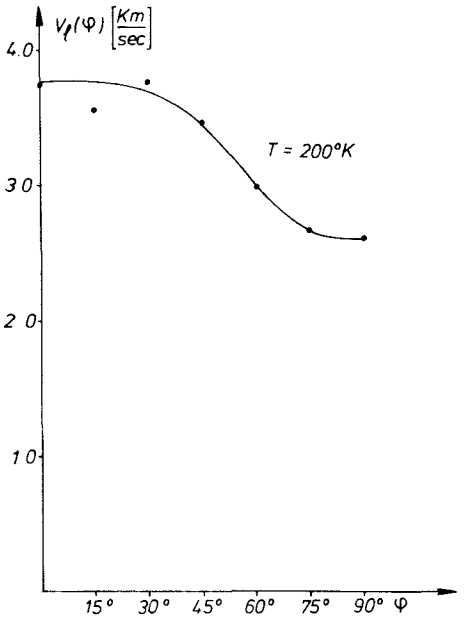

FIG. 19. Phonon velocities as a function of φ obtained from the temperature dependent part of $\lim_{s\to 0} (1/N)I(s,\varphi)$.

mean that either the short-range order is not of a bundle type, or if it is of this type, that the disorder in the packing is about as large as the disorder in the structure of the chains which form the rodlike structural units.

The anisotropy appearing at higher temperatures is related to the anisotropy

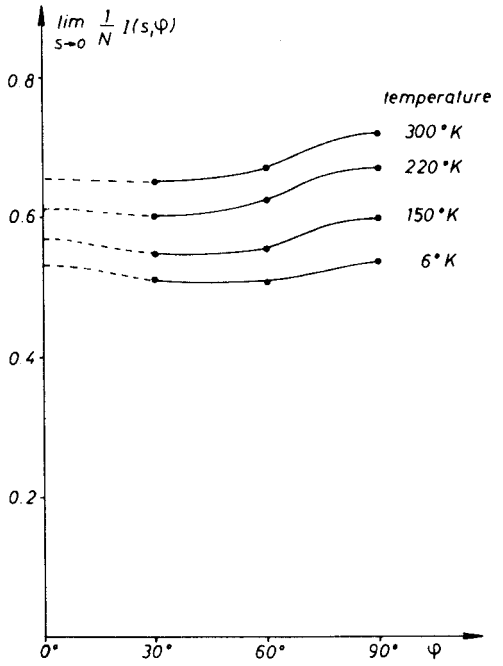

FIG. 20. Diffuse X-ray scattering of an oriented PET film extrapolated towards zero scattering angle as a function of φ for four different temperatures.

of thermal motion due to longitudinal vibration of long wavelength. It can be used to calculate the direction dependence of the group velocities of these vibrations which are shown in Figure 19.

Preliminary studies on an anisotropic sample of polyethyleneterephthalate (Fig. 20) show a not entirely vanishing anisotropy at very low temperatures which could be taken as an indication for small anisotropy in the short-range order. However, more detailed studies on a larger number of samples are necessary before more definite statements can be made.

REFERENCES

[1] R. J. Roe, *J. Appl. Phys.*, **36**, 2024 (1965).
[2] Laue, M. von, *Z. Kristallogr.*, **82**, 127 (1932).
[3] W. Ruland, *J. Appl. Phys.*, **38**, 3585 (1967).
[4] W. Ruland, and H. Tompa, *Acta Crystallogr.*, **A24**, 93 (1968).
[5] O. J. Guentert, and S. Cvikevich, *Carbon*, **1**, 309 (1964).
[6] A. Fourdeux, R. Perret and W. Ruland, *J. Appl. Crystallogr.*, **1**, 252 (1968).
[7] J. Rathje, and W. Ruland, *Coll. Polym. Sci.*, **254**, 358 (1976).